Journal of Magnetic Resonance 212 (2011) 311–319

Contents lists available at ScienceDirect

Journal of Magnetic Resonance

journal homepage: www.elsevier.com/locate/jmr

Multiple resonance heteronuclear decoupling under MAS: Dramatic increase of spectral resolution at moderate magnetic field and MAS frequencies

Charlotte Martineau [a,*], Franck Engelke [b], Francis Taulelle [a]

[a] Tectospin, Institut Lavoisier de Versailles (ILV), UMR CNRS 8180, Université de Versailles Saint-Quentin-en-Yvelines, 45 Avenue des États-Unis, 78035 Versailles cedex, France
[b] Bruker BioSpin GmbH, Silberstreifen 4, D-76287 Rheinstetten, Germany

ARTICLE INFO

Article history:
Received 12 May 2011
Revised 13 July 2011
Available online 23 July 2011

Keywords:
Hetero-nuclear decoupling
High-resolution
Multiple-irradiation probe
Optimized T_2
2D NMR

ABSTRACT

The effects of multiple-resonance heteronuclear decoupling under magic angle spinning (MAS) on the resolution of one-dimensional ^{19}F and ^{31}P and various two-dimensional MAS NMR spectra and on the residual non-refocusable coherence lifetimes in fluorinated aluminophosphate $AlPO_4$-CJ2, *i.e.* a compound that contains numerous highly abundant nuclei but no homonuclear spin bath, has been investigated. The design of the four-channel (^1H, ^{19}F, ^{27}Al, ^{31}P) MAS probe used for this study is first described. ^1H and ^1H–^{27}Al double-resonance decouplings allows lengthening the optimized transverse relaxation T_2^{opt} and increasing the resolution in the ^{19}F and ^{31}P dimensions. Under the application of multi-nuclear decoupling, a two-dimensional ^{19}F–^{31}P CP-HETCOR correlation spectrum for $AlPO_4$-CJ2 is recorded with unprecedented high-resolution in the two dimensions. Moreover, because ^1H-decoupling increases the ^{19}F T_2^{opt}, it has been applied during the entire duration of the 2D NMR experiments, allowing the direct use of residual small interactions to generate ^{19}F–^{19}F and ^{19}F–^{27}Al 2D NMR correlation spectra in $AlPO_4$-CJ2.

1. Introduction

Solid-state nuclear magnetic resonance (NMR) methods combined with magic angle spinning (MAS) have greatly improved over the past decades, including the development of numerous decoupling and magnetization transfer schemes, as well as two-dimensional (2D) correlation techniques, based either on homonuclear or heteronuclear, dipolar or scalar interactions. While the dipolar interaction yields features about through space proximities, the scalar interaction, mediated through chemical bonds, contains information about the connectivity between nuclei [1]. Although the scalar interaction is usually of several orders of magnitude lower than the dipolar interactions and often hindered by the spectral linewidth, it has emerged, along with the improvement of high-resolution techniques, as a complementary method to the dipolar correlation [2,3]. Indeed, it is not the transverse coherence lifetime given by the experimental linewidth that is the actual limitation in the use of such small couplings, but the residual non-refocusable one T_2'. T_2' is a function dependant on the MAS frequency and the decoupling scheme(s) to which the sample is submitted and that more or less efficiently scale down the spin–spin interactions. To generate a 2D NMR correlation spectrum, T_2' has to be optimized by a proper choice of experimental conditions (adjustment the MAS frequency, selectively reintroduction or decoupling of interactions, etc) so that the resulting optimized T_2^{opt} of the concerned nuclei becomes longer than the time required by the interaction carrying the targeted information to build-up. The T_2^{opt} is also related to the spectral resolution, and therefore, to reach high-resolution performances, interactions that contribute to a decrease of T_2^{opt} must be removed. For example, homonuclear dipolar decoupling schemes involving combined rotation and multiple pulse spectroscopy (CRAMPS), by reducing the ^1H–^1H dipolar interaction, contribute to decrease the transverse relaxation [4].

In solid inorganic fluorinated compounds, heteronuclear *J*-couplings involving the ^{19}F nucleus ranging from hundred to thousands of Hz have been reported, like, for example, in the case of the ^{19}F–^{31}P [5,6], ^{19}F–$^{69,71}Ga$ [7], ^{19}F–^{75}As [8], ^{19}F–^{93}Nb [9,10], ^{19}F–^{115}In [11], ^{19}F–^{119}Sn [12,13] or ^{19}F–^{207}Pb [14–19] spin pairs. Providing an efficient averaging of the ^{19}F homonuclear interaction thus a prolonged ^{19}F T_2' (*i.e.* under fast MAS in hydroxyfluorides or oxyfluorides or under ultra-fast MAS in inorganic fluorides), smaller interactions that survive MAS, like homonuclear ^{19}F–^{19}F isotropic *J*-couplings or ^{19}F homogeneous homonuclear dipolar Hamiltonian, can be used to generate 2D double-quantum single-quantum (DQ–SQ) NMR spectra, as was done, for example in a deuterated-hydroxyfuorinated silicate [20] (for which the ^1H–^{19}F dipolar couplings could also be neglected) or in inorganic fluorides [21].

In our work, we were faced to $AlPO_4$-CJ2 [22], a compound belonging to the class of microporous crystalline fluorinated aluminophosphate [23], which are materials containing numerous

* Corresponding author.
E-mail address: charlotte.martineau@chimie.uvsq.fr (C. Martineau).

1090-7807/$ - see front matter © 2011 Elsevier Inc. All rights reserved.
doi:10.1016/j.jmr.2011.07.012

NMR-accessible nuclei (^{1}H, ^{19}F, ^{27}Al, ^{31}P). If these solids are usually free from strongly homonuclear dipolar-coupled spins (*i.e.* no ^{1}H or ^{19}F spin-baths), the presence of abundant nuclei induces heteronuclear couplings (dipolar and scalar) responsible for NMR spectral resolution loss. For the purpose of this study, a four-channel (^{1}H, ^{19}F, ^{27}Al, ^{31}P) MAS probe was built, whose design concepts are presented in the first section of the paper. Then, we present the optimization of the T_2^{opt} (for both gain in signal and resolution), and the extended possibility of solid-state NMR experiments that can be applied to this class of compounds, by application of multiple resonance heteronuclear NMR techniques. In particular, the influence of single ^{1}H or double-resonance ^{1}H and ^{27}Al heteronuclear decoupling, under moderate MAS frequency conditions (10–15 kHz), on the resolution of the ^{19}F and ^{31}P NMR spectra of fluorinated aluminophosphate $AlPO_4$-CJ2 is evaluated. Since these decoupling schemes also significantly increase the coherence lifetime T_2^{opt}, we show that their application during both the acquisition periods of the signals and the periods of excitation of the multiple-quantum coherences yields ^{19}F–^{31}P 2D NMR spectra with unprecedented spectral resolution, and allows the use of small ^{19}F–^{19}F residual interactions and, for the first time, ^{19}F–^{27}Al *J*-couplings to generate 2D correlation MAS NMR spectra in $AlPO_4$-CJ2.

2. Experimental

2.1. Sample

$AlPO_4$-CJ2 was synthesized by hydrothermal synthesis as described in reference [24]. The purity of the sample was controlled by powder X-ray diffraction.

2.2. NMR experiments

All NMR experiments were performed on an Avance 500 Bruker spectrometer (static magnetic field B_0 = 11.7 T, Larmor frequencies of 500.1, 470.6, 202.5 and 130.3 MHz for ^{1}H, ^{19}F, ^{31}P and ^{27}Al, respectively). ^{1}H, ^{19}F, ^{31}P and ^{27}Al simultaneous quadruple-irradiation was achieved using a quadrupole resonance 2.5 mm cross-polarization magic angle spinning (CP-MAS) probe. In this probe, ^{1}H and ^{19}F frequencies are combined to travel through the same channel, but with separated tuning for each frequency.

The ^{19}F Hahn-echo NMR spectra were recorded in the 15–30 kHz MAS range, using 2.5 μs 90° pulses, inter-pulse delays synchronized with the rotor frequency and recycle delays of 10 s. When mentioned, a ^{1}H 64-step small-phase incremental alteration (SPINAL-64) [25] decoupling (nutation frequency of 90 kHz) was implemented in the acquisition period of the ^{19}F MAS spectrum.

The ^{1}H–^{31}P cross-polarization [26,27] (CP) MAS (15 kHz) NMR spectra of $AlPO_4$-CJ2 were recorded using a 2.85 μs initial ^{1}H 90° pulse length, a 5 ms contact time, 5 s recycle delay, and accumulation of 16 transients. A ^{1}H RAMped amplitude (RAMP)-CP [28] contact pulse was employed, with a RF field centered on the n = +1 Hartmann–Hahn matching condition (*i.e.* $\nu_{RF}(^1H) = \nu_{RF}(^{31}P) + \nu_{ROT}$) and spanning over $\pm\nu_{ROT}$, with $\nu_{RF}(^{31}P)$ = 62.5 kHz and ν_{ROT} = 15 kHz. When mentioned, ^{1}H SPINAL-64 decoupling (nutation frequency of 90 kHz) and ^{27}Al rotor-asynchronized multi-pulses (RA-MP) [29] decoupling (nutation frequency of 30 kHz) were implemented during the acquisition of the ^{31}P signal.

The ^{19}F–^{27}Al heteronuclear multiple-quantum correlation (*J*-HMQC) [30] NMR correlation spectrum of $AlPO_4$-CJ2 was recorded at MAS frequency of 15 kHz. In the *J*-HMQC, 11 μs 90° pulse length were employed on ^{27}Al, and the excitation of the double-quantum coherence was synchronized with the rotor frequency and set to 2.67 ms. Eighty t_1 slices with 64 transients each were accumulated. ^{1}H SPINAL-64 decoupling was implemented during the excitation periods as well as during the acquisition of the ^{19}F signal.

The ^{19}F–^{31}P CP heteronuclear correlation (CP-HETCOR) NMR spectrum of $AlPO_4$-CJ2 was recorded at MAS frequency of 15 kHz, using a 6 ms contact time. ^{1}H SPINAL-64 decoupling was implemented during the whole experiment. ^{27}Al RA-MP decoupling

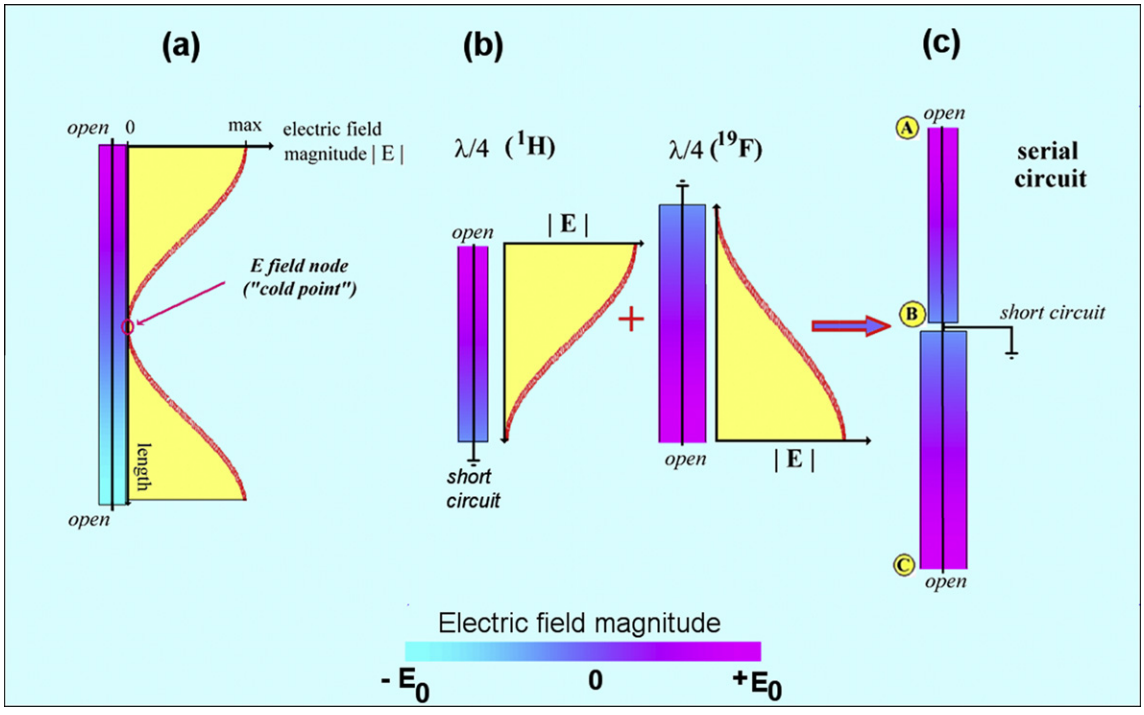

Fig. 1. Homogeneous line resonator (a) modified in a way (b) such that it becomes a heterogeneous line resonator (c). The color bars indicate the electric field amplitude along the coaxial transmission line. The magnitude is drawn over the field amplitude (color bar). At the open ends of the line resonator the electric field magnitude is maximum, while in the center of the homogeneous line resonator or at points short-circuited to ground the electric field is zero. (For interpretation of the references to colour in this figure legend, the reader is referred to the web version of this article.)

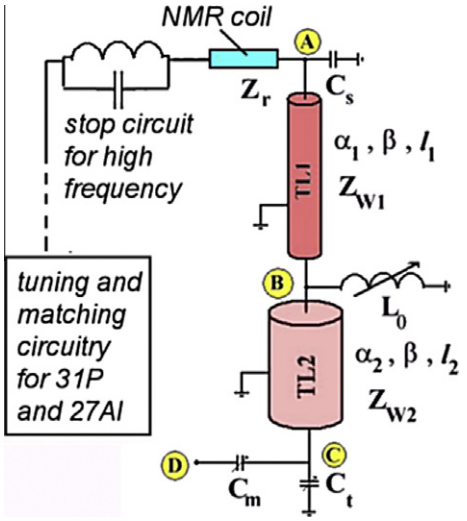

Fig. 2. $^1H/^{19}F$ circuit consisting of the heterogeneous coaxial transmission line resonator (TL1 + TL2), now surrounded by cylindrical tubular shield, with splitting inductance L_0 introduced at the cold point of the line resonator. α_i, β_i, l_i, and Z_{wi} denote the loss factor, propagation factor, length, and characteristic impedance of the ith subunit ($i = 1, 2$) forming the heterogeneous line resonator.

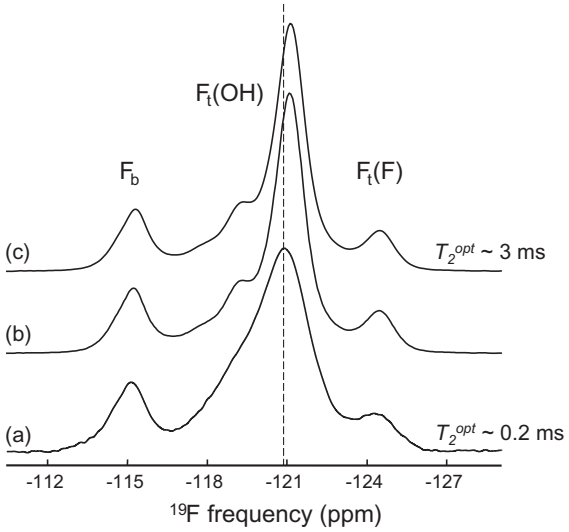

Fig. 3. ^{19}F NMR spectra of $AlPO_4$-CJ2 recorded (a) without decoupling at MAS 30 kHz, and with ^1H SPINAL decoupling at (b) MAS 30 kHz and (c) MAS 15 kHz. The vertical dash line is a guide for the eye.

was additionally implemented during the acquisition of the ^{31}P signal. Eighty t_1 slices with 128 transients each were accumulated.

The ^{19}F double-quantum single-quantum [31] (DQ–SQ) NMR spectra of $AlPO_4$-CJ2 was recorded at MAS frequency of 15 kHz. The DQ coherence was generated through the dipolar homonuclear homogeneous Hamiltonian (DH^3) experiment [21], whose pulse sequence is identical to that of the Refocused incredible natural abundance double quantum transfer (R-INADEQUATE) [2] experiment. The rotor-synchronized delay to excite the DQ coherence was set to 1 ms. ^1H SPINAL-64 decoupling (90 kHz) was during the acquisition of the ^{19}F signal in both horizontal and vertical dimensions as well as during the DQ excitation delays.

In all 2D NMR experiments, phase sensitive detection in the indirect dimension was obtained using the States [32] method. The ^{19}F, ^{31}P and ^{27}Al chemical shifts were referenced to $CFCl_3$, H_3PO_4 85% and a 1 M solution of $Al(NO_3)_3$, respectively. The spectra were reconstructed using the Dmfit [33] software.

3. Results and discussion

3.1. Design of the four-channel probe

In order to study simultaneously the whole four-spin system (^1H, ^{19}F, ^{27}Al, ^{31}P) in the fluorinated aluminophosphate $AlPO_4$-CJ2, building a corresponding four-channel MAS probe was necessary. The first design of a more than one additional channel probe has been given by Schaefer [34] with a six-irradiation channel probe. More recently, Limbach et al. presented a five-channel probe for biological samples [35]. The specific task to realize ^1H and ^{19}F frequencies in one circuit has been addressed by various research groups [36,37]. Here we describe a different technique as published in [38] based on transmission line resonators. The concept of a standing electromagnetic wave on a coaxial transmission line resonator is illustrated in Fig. 1. First, in Fig. 1a, a two-sided open transmission line resonator with a standing wave of a half wavelength $\lambda/2$ equal to the geometric length l of the line is shown. The electric field magnitude is maximum at both open ends of the line and is equal to zero at the center of the line, in technical jargon this latter point is referred to as "cold point". The homogeneous coaxial line of Fig. 1a is cut conceptually into two parts as shown in Fig. 1b with short-circuiting the cold point. The outer diameter and the length l_1 of one of the two parts of the coaxial line is now changed yielding a different characteristic impedance Z_{W1} and a different quarter wavelength $\lambda_1/4 = l_1$ compared to the other part of length l_2 with characteristic impedance Z_{W2}. Reassembling the two parts as shown in Fig. 1c gives an heterogeneous coaxial line resonator with the cold point not necessarily located in the center anymore. A real short circuit of the cold point B does not affect the distribution of the electric field along the line between the points A and C. In contrast to the homogeneous $\lambda/2$ line resonator of Fig. 1a, which has the resonance frequency $f = c/\lambda$, the heterogeneous line resonator of Fig. 1c reveals two resonance frequencies f_1 and f_2 that now depend on the lengths l_1 and l_2 as well as on the characteristic impedances Z_{W1} and Z_{W2}.

In order to make use of the heterogeneous line resonator for designing a probe circuitry that exhibits nearby resonance frequencies as for ^{19}F and ^1H, the structure of Fig. 1c needs to be embedded in a suitable tune and match circuit. An example [38] is represented in Fig. 2. The upper end A of the resonator (see Figs. 1c and 2) is connected to the NMR RF coil with complex impedance Z_r. The capacitance C_s represents a stray capacitance caused by the feed-throughs of the resonator. At the cold point B in Fig. 2 the short circuit of Fig. 1c is replaced by a variable inductance L_0 to fine-tune the resonances f_1 and f_2. The lower end C of the resonator is terminated by a tuning capacitance C_t, and between point C and the capacitance C_t the RF is fed in and out in point D in series with the matching capacitor C_m.

On the opposite side of the NMR coil a tank circuit consisting of a parallel LC circuit acts as a high-frequency stop circuit providing a high impedance for the ^{19}F and ^1H frequency. On the other side of this $^1H/^{19}F$ stop circuit the conventional $^{27}Al/^{31}P$ circuit is connected, comprising tuning capacitances for the ^{31}P and ^{27}Al channel in series to the NMR coil Z_r, another LC stop circuit (in the ^{27}Al channel tuned to ^{31}P) to decouple the ^{31}P channel from the ^{27}Al channel, and variable inductances connected to ground to match these channels to 50 Ω.

The probe circuit thus built provides four different resonance frequencies (^1H, ^{19}F, ^{31}P, ^{27}Al) on three external ports – two separate ports for ^{27}Al and ^{31}P and one common port for ^1H and ^{19}F (port D in Fig. 2). In order to separate ^1H and ^{19}F channels from each other, a diplexer (a kind of impedance matched T circuit) is

connected to the $^{1}H/^{19}F$ port, providing a 50 Ω impedance to the probe port and 50 Ω each for the ^{1}H and for the ^{19}F channel. Each branch of the diplexer output is followed by either ^{1}H pass/^{19}F stop highpass filters (in the ^{1}H channel) or by ^{19}F pass/^{1}H stop bandpass filters (in the ^{19}F channel). These highpass and bandpass filters finally yield a channel separation of more than 85 dB such that experiments like ^{19}F observation under simultaneous ^{1}H decoupling become possible. Once tuned and matched for each channel, the probe can simultaneously deliver RF field amplitudes (or equivalently, RF efficiencies) of 100 kHz (ca. 16 kHz/$(W)^{1/2}$) for ^{1}H, 80 kHz for ^{19}F (ca. 13 kHz/$(W)^{1/2}$), 70 kHz (ca. 7 kHz/$(W)^{1/2}$) for ^{31}P, and 60 kHz (ca 5 kHz/$(W)^{1/2}$) for ^{27}Al for long decoupling pulses.

3.2. Application to $AlPO_4$-CJ2

The structural build unit (SBU) of $AlPO_4$-CJ2 contains one six-coordinated and one five-coordinated aluminum and two four-fold phosphorus inequivalent sites [24]. In each SBU, the aluminum and phosphorus sites are alternated to form a square-like unit. The penta-coordinated aluminum shares a bridging group with the hexa-coordinated aluminum, which also has a bond to a terminal site. While the terminal site is fully occupied by a F atom, the bridging site can be either a OH group (named SBU-OH, 67% probability) or a F atom (named SBU-F, 33% probability). Previous NMR experiments have shown the sensitivity of the ^{19}F, ^{31}P and ^{27}Al isotropic chemical shift to the kind of chemical group on the bridging position (OH group of F atom), and the various 1D and 2D NMR spectra have pointed towards a random distribution of the SBUs in the solid network [39].

3.2.1. 1D MAS NMR spectra

The ^{19}F Hahn-echo MAS (30 kHz) NMR spectrum of $AlPO_4$-CJ2 (Fig. 3a) shows three main resonances located at isotropic chemical shift (δ_{iso}) of −115, −121 and −124 ppm, which have been previously assigned to the three inequivalent fluorine atoms in SBU [39]: the bridging F atom (F_b), the terminal F atom in a SBU-OH (F_t(OH)) and the terminal F atom in a SBU-F (F_t(F)), respectively. Because $AlPO_4$-CJ2 contains protons (NH_4^+ molecules in the pores and a crystallographic site partially occupied by an OH-group), application of ^{1}H SPINAL-64 decoupling (^{1}H decoupling RF field corresponding to a 90 kHz nutation frequency) during the echo and evolution periods of the ^{19}F signal leads to an increase of the ^{19}F T_2^{opt} measured from the Hahn-echo decay (from ∼0.4 ms to ∼3 ms) and results in an better resolved ^{19}F NMR spectrum (Fig. 3b) as compared to a spectrum recorded without decoupling at a fast-MAS of 30 kHz (Fig. 3a). One can notice a slight shift (∼−0.5 ppm, c.a. 235 Hz) of the ^{19}F resonances upon ^{1}H decoupling, due to Bloch–Siegert [40] effect between ^{1}H and ^{19}F which have close Larmor frequencies (29.5 MHz (6%) difference at B_0 = 11.7 T). At lower MAS frequency of 15 kHz (Fig. 3c), the resolution of the ^{1}H-decoupled ^{19}F MAS NMR spectrum is similar to that recorded at MAS 30 kHz, indicating that for $AlPO_4$-CJ2, in which the F atoms are 'diluted' (there are either isolated F atoms in the SBU-OH or pairs of fluorine atoms in the SBU-F), the ^{19}F–^{19}F homonuclear dipolar interaction is already averaged out at moderate MAS frequency of 15 kHz. This situation is different from that observed in purely fluorinated inorganic solids, in which the strongly coupled ^{19}F spin system is very difficult to decouple, even using ultra-fast MAS [41]. ^{1}H-decoupling allows resolution of two extra lines on the ^{19}F MAS NMR spectrum of $AlPO_4$-CJ2, located at −118 and −119 ppm, which suggests the occurrence of several different chemical environments for these fluorine atoms. This multiplicity of the magnetically inequivalent environments around the fluorine atoms can be related to the repartition of the SBU-OH and SBU-F in the solid network of $AlPO_4$-CJ2.

The ^{1}H–^{31}P CP–MAS (10 kHz) NMR spectrum of $AlPO_4$–CJ2 (Fig. 4a) shows two main resonances of equal relative intensity, centered around – 10 ppm and – 20 ppm previously assigned, based on their isotropic chemical shift to the two inequivalent phosphorus atoms P2 and P1 of the structure, respectively [39]. Each of the two ^{31}P resonances has a shoulder, whose resolution

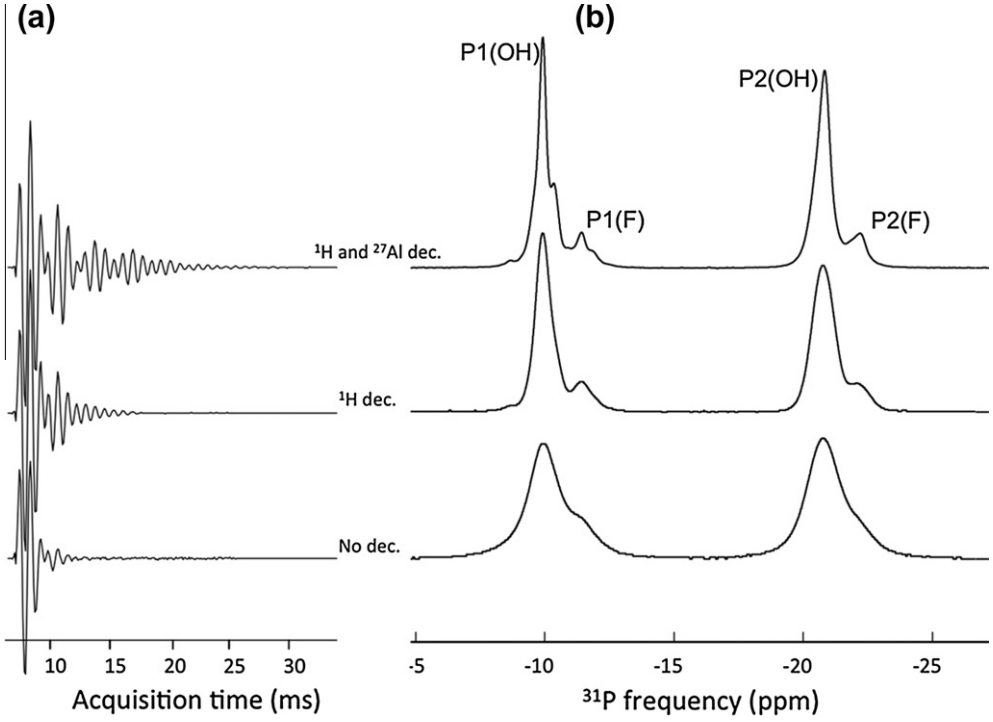

Fig. 4. (a) Free induction decay and (b) NMR spectrum obtained after Fourier Transform for ^{1}H–^{31}P CP-MAS (10 kHz) NMR experiments of $AlPO_4$-CJ2 recorded without decoupling, with ^{1}H-SPINAL decoupling and with ^{1}H-SPINAL and ^{27}Al-RA-MP decoupling schemes.

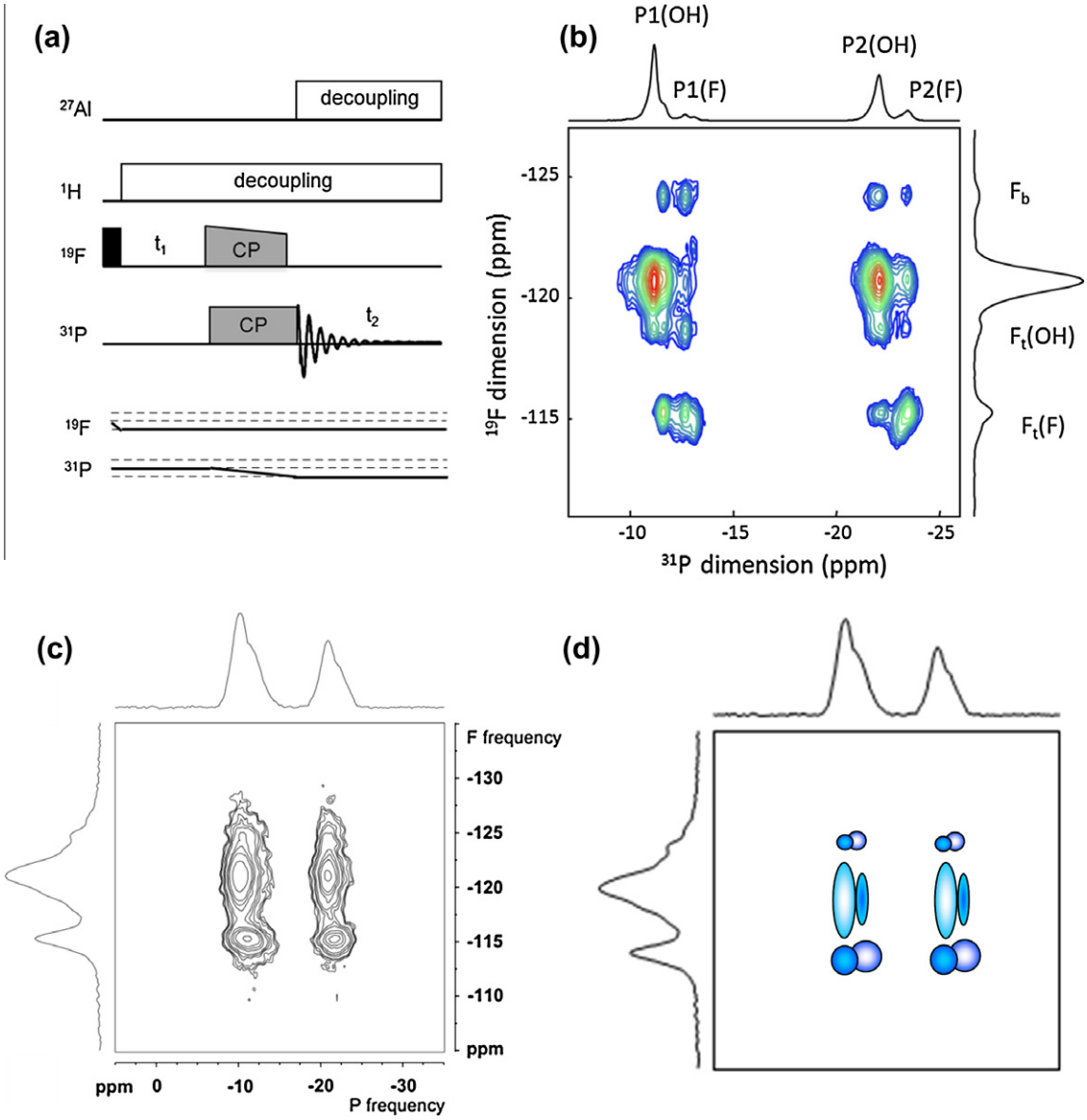

Fig. 5. ^{19}F–^{31}P CP-HETCOR (a) pulse sequence and (b) corresponding MAS (15 kHz) 2D NMR correlation spectrum of $AlPO_4$-CJ2. The top and right spectra, on which lines are assigned, are the full projections along the horizontal and vertical dimensions, respectively. The dash lines indicate P–F correlations. (c) ^{19}F–^{31}P CP-HETCOR NMR spectrum recorded without any decoupling, taken from ref [39]. (d) The spectrum in (c) had been described as compatible with a virtual 2D for which full disorder of building units was assumed. The spectrum (a) clearly confirms this deduction.

can be increased by application of 90 kHz RF field ^1H-SPINAL decoupling and significantly further increased by application of double-resonance ^1H-SPINAL and ^{27}Al moderate power (30 kHz RF field) RA-MP decoupling (Fig. 4b). Along with the improved resolution, the duration of the ^{31}P free induction decay, thus the T_2^{opt}, is also significantly increased upon heteronuclear multi-resonance decoupling (Fig. 4a). Additional ^{19}F SPINAL-64 decoupling has no apparent influence on the ^{31}P NMR spectrum, either because the ^{31}P line widths were already reduced to the point where the chemical shifts distribution represent the limit in resolution or because the combination of ^{19}F dipolar and CSA interactions decreases the efficiency of the SPINAL-64 scheme. Two main resonances for each P1 and P2 atoms can be distinguished, which correspond to P1 and P2 in a SBU-F and OH (labeled P(F) and P(OH), respectively). Each of these sub-peaks also has several contributions, which can also be related to the distribution of SBUs around one given SBU in this compound [39].

Suppression (or strong reduction) of heteronuclear interactions (^1H–^{19}F, ^1H–^{31}P, ^{27}Al–^{31}P) in fluorinated aluminophosphate can be achieved using single or double heteronuclear decoupling schemes, even at moderate MAS frequency and B_0 magnetic field, yielding increased T_2^{opt} for ^{19}F and ^{31}P and high-resolution NMR spectra can be obtained. The ^{31}P chemical shifts definitively seem to be the more sensitive to slight structural disorder observed in $AlPO_4$-CJ2.

3.2.2. 2D MAS NMR spectra

3.2.2.1. ^{19}F–^{31}P. ^{19}F–^{31}P spatial proximities have been probed using the CP-HETCOR experiment at moderate MAS frequency (15 kHz). As previously mentioned, high-resolution in both direct ^{31}P and indirect ^{19}F dimensions required the suppression of all heteronuclear couplings (^1H–^{19}F, ^1H–^{31}P, ^{27}Al–^{31}P) by application of ^1H decoupling during the acquisition of the ^{19}F signal and both ^1H and ^{27}Al decoupling during the acquisition of the ^{31}P signal

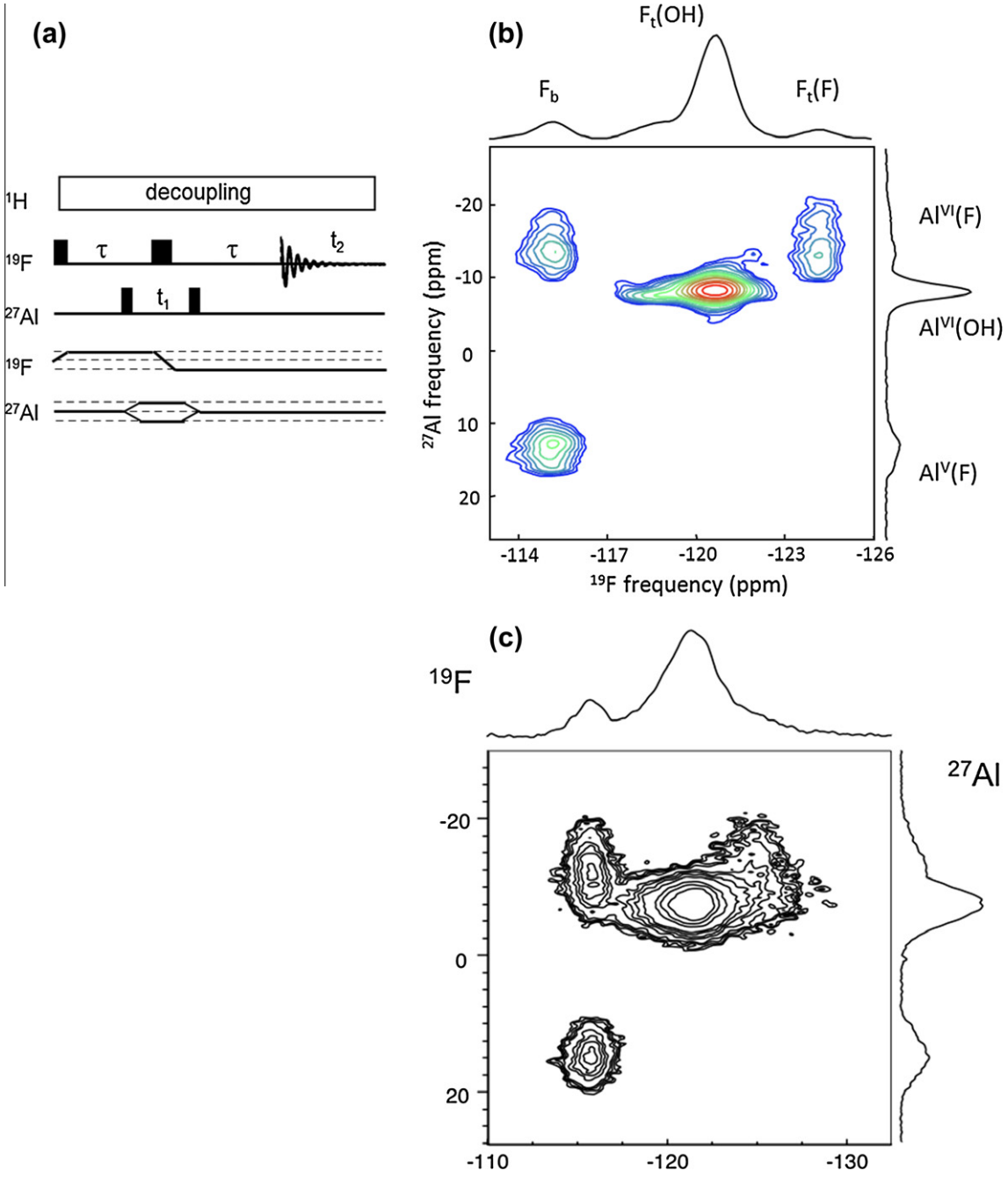

Fig. 6. ^{19}F–^{27}Al *J*-HMQC (a) pulse sequence and (b) corresponding MAS (15 kHz) 2D NMR correlation spectrum of $AlPO_4$-CJ2. The top and right spectra, on which lines are assigned, are the full projections along the horizontal and vertical dimensions, respectively. The dash lines indicate F–Al correlations. (c) ^{19}F–^{27}Al 2D correlation MAS NMR spectrum recorded with the CP-HETCOR pulse sequence and without any decoupling, taken from ref [39].

(Fig. 5a). The obtained ^{19}F–^{31}P CP-HETCOR MAS (15 kHz) NMR correlation spectrum of $AlPO_4$-CJ2 (Fig. 5b) indeed shows a resolution on both dimensions much better than what was obtained earlier (Fig. 5c) under equivalent magnetic field (11.7 T) and MAS frequency (∼15 kHz) but without any decoupling. The observed cross-correlations peaks between P1(F)–P2(F) and P1(OH)–P2(OH) indicate proximities between the P and F atoms within a SBU, while the cross-correlation P1(F)–P2(OH) and P1(OH)–P2(F) indicate proximities between phosphorous atoms belonging to neighboring SBUs. The presence of cross peaks between P from SUB-OH(F) and F from SBU-F (resp. OH) confirms the random character of the distribution of the SBUs in the solid network, rather than a separation in distinct domains (Fig. 5d).

3.2.2.2. ^{19}F–^{27}Al. Proximities between the fluorine and aluminum atoms in fluorinated samples are usually probed though the heteronuclear dipolar interaction in CP experiments [42–45], which can be tricky to set-up and are sensitive to offsets because of the quadrupolar spin ^{27}Al (I = 5/2). ^{19}F–$^{69,71}Ga$ [7] and ^{19}F–^{115}In [11] *J*-couplings of c.a. 100s of Hz have been measured in the solid-state. Therefore, although it has to date never been measured, similar values can also be expected for the ^{19}F–^{27}Al spin pair. In $AlPO_4$-CJ2, around 3 ms time was required for the ^{19}F–^{27}Al heteronuclear double-coherence to build-up (*i.e.* longer than the ^{19}F T_2^{opt} without application of ^{1}H decoupling). Therefore signal through the ^{19}F–^{27}Al *J*-HMQC experiment could only be obtained under application of ^{1}H-decoupling during the excitation periods of this

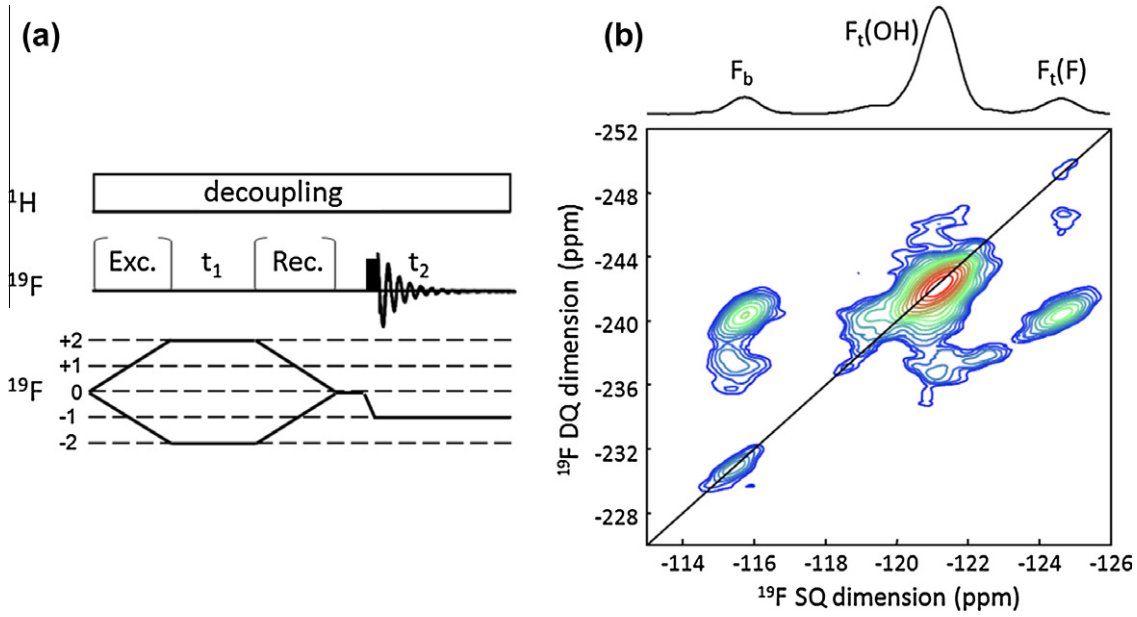

Fig. 7. ^{19}F–^{19}F DQ–SQ (a) pulse sequence and (b) corresponding MAS (15 kHz) 2D NMR correlation spectrum of $AlPO_4$-CJ2. The excitation of the DQ coherence was achieved using the DH^3 scheme [21], identical to the five-pulse R-INADEQUATE [30] experiment. The top spectrum, on which lines are assigned, is the full projection along the horizontal dimensions. The thick line indicates the diagonal with slope of 2. The dash lines indicate F–F correlations.

double-coherence (Fig. 6a). In addition, to get high-resolution ^{19}F direct dimension, ^{1}H decoupling was also applied during the acquisition of the ^{19}F signal. In the case of $AlPO_4$-CJ2, the ^{19}F line width is mostly homogeneous and due to coupling with the ^{1}H. Thus, the ^{1}H decoupling results in both an increased efficiency of the *J*-based transfer and a gain in resolution in the ^{19}F dimension. The resulting ^{19}F–^{27}Al *J*-HMQC MAS (15 kHz) NMR spectrum of $AlPO_4$-CJ2 is shown in Fig. 6b. Again, the resolutions in both dimensions are much better than what was obtained earlier on a ^{19}F–^{27}Al CP-HETCOR NMR spectrum (Fig. 6c) under equivalent magnetic field (11.7 T) and MAS frequency (∼15 kHz) but without any decoupling. It should be mentioned that these heteronuclear experiments could be combined with a high-resolution multiple-quantum (MQ-MAS) filter in the ^{27}Al indirect dimension [46–48] to even further the gain in resolution. Finally, the observed connectivity pattern on the 2D NMR spectrum evidences the difference between the fluorinated SBUs which contains bridging F site (F_b) linking two aluminum sites, and the hydroxylated SBUs, in which only one F atom is linked to a six-fold coordinated aluminum site.

3.2.2.3. ^{19}F–^{19}F. Fluorine–fluorine proximities can conveniently be probed using DQ–SQ NMR experiments, with the ^{19}F–^{19}F homonuclear dipolar coupling, very strong in inorganic fluorides, being the sourced interaction used to generate the DQ coherence. Since it is partially averaged out by MAS, the homonuclear dipolar interaction must be reintroduced by means of, for example, the BABA [49] or SPIP [50] recoupling pulse sequences [18,19,41,51–54]. However, it has recently been shown that small (20–80 Hz) *J*-couplings [20] or the homogeneous homonuclear dipolar Hamiltonian that are not averaged out by MAS [21], can also be directly used, *i.e.* without any recoupling, in the R-INADEQUATE [30] or DH^3 [21] NMR experiments, respectively. One limitation in the use of such small interactions (compared to the dipolar interaction) is the longer time needed for the DQ coherence to build-up (1–10 ms in the R-INADEQUATE *vs* 100s of μs in a dipolar driven experiment), which therefore requires long ^{19}F coherence lifetime T_2^{opt}. In deuterated oxyfluorides [20] this can be achieved using fast MAS (30 kHz) since the F atoms are far from each other and not coupled to any protons. In pure fluorides [21], the ^{19}F–^{19}F dipolar interaction has to be efficiently averaged out, which can be done under ultra-fast MAS (60–70 kHz) conditions. In $AlPO_4$-CJ2, which does not contain strongly coupled homonuclear spin systems, optimized T_2^{opt} is obtained when the ^{19}F–^{1}H dipolar interaction is averaged out, *i.e.* either under ultra-fast MAS conditions or, as in our case, under ^{1}H-decoupling at moderate MAS. Consequently, maximum ^{19}F DQ signal intensity was obtained in the DH^3 experiment with application of ^{1}H-decoupling during the DQ excitations periods (Fig 7a). In addition ^{1}H-decoupling was also applied during the ^{19}F signal detection to obtain high-resolution dimensions. The resulting ^{19}F–^{19}F DH^3 spectrum of $AlPO_4$-CJ2 (Fig. 7b) shows expecting cross-correlation peaks between neighboring F atoms within a structural unit (F_b–F_t(F)), as well as longer range correlations between F atoms in neighboring structural units (F_b–F_t(OH), F_b–F_b, F_t(F)–F_t(OH), F_t(F)–F_t(F)).

4. Conclusions

The effect of multiple-resonance heteronuclear decoupling under MAS on the resolution of 1D ^{19}F and ^{31}P and various 2D MAS NMR spectra and on the coherence lifetimes T_2^{opt} in fluorinated aluminophosphate $AlPO_4$-CJ2, *i.e.* a compound that contains numerous highly abundant nuclei but no homonuclear spin bath, has been investigated. The use of relaxation to improve resolution has previously been considered in the liquid-state in the transverse relaxation optimization spectroscopy (TROSY) NMR experiment [55]. Although the set of interactions are much more complex in the solid-state, using multiple RF irradiations may potentially also lead, by selective suppression of interactions, to comparable effects under MAS. If only one pair of interactions could be retained, then by multi-radio-frequency-decoupling, one might access TROSY under MAS (mrfd-TROSY-MAS). ^{1}H decoupling and double-resonance ^{1}H–^{27}Al increases both the resolution and the T_2^{opt} of ^{19}F and ^{31}P, respectively. A quadruple frequencies probe (^{1}H, ^{19}F, ^{27}Al, ^{31}P) allows obtaining two-dimensional ^{19}F–^{31}P CP-HETCOR correlation spectrum for $AlPO_4$-CJ2 with high-resolution in the two dimensions. Because ^{1}H-decoupling increases the ^{19}F T_2^{opt}, it has

been applied during the whole 2D NMR experiments. Under these conditions, small interactions like ^{19}F residual dipolar couplings and ^{19}F–^{27}Al *J*-couplings, have been directly used to generate ^{19}F–^{19}F and ^{19}F–^{27}Al 2D NMR correlation spectra in $AlPO_4$-CJ2. The various NMR spectra of $AlPO_4$-CJ2 displayed in this contribution show that manipulating the relaxation times provides significant gains in sensitivity and a resolution about 2.5 higher than what could have been achieved by increasing the static magnetic field from 11.7 T to 23.4 T. This consequence indicates that considerable improvements in resolution enhancement could be undertaken at moderate magnetic fields with multiple channels probes.

Acknowledgments

CM thanks Dr. Thierry Loiseau (UCCS, Lille) and Dr. Mohamed Haouas (ILV, Versailles) who provided the $AlPO_4$-CJ2 sample and Dr. Franck Fayon (CEMHTI, Orléans) for helpful discussions.

References

[1] J. Varaa, J. Jokisaari, R.E. Wasylishen, D.L. Bryce, Spin–spin coupling tensors as determined by experiment and computational chemistry, Prog. Nucl. Magn. Reson. Spectrosc. 41 (2002) 233–304.
[2] A. Lesage, M. Bardet, L. Emsley, Through-bond carbon–carbon connectivities in disordered solids by NMR, J. Am. Chem. Soc. 121 (1999) 10987–10993.
[3] D. Lee, J. Struppe, D.W. Elliott, L.J. Mueller, J.J. Titman, Sensitive absorptive refocused scalar correlation NMR spectroscopy in solids, Phys. Chem. Chem. Phys. 11 (2009) 3547–3553.
[4] A. Lesage, L. Duma, D. Sakellariou, L. Emsley, Improved resolution in proton NMR spectroscopy of powdered solids, J. Am. Chem. Soc. 123 (2001) 5747–5752.
[5] M. Weil, M. Purchberger, E. Fulgeinm, E.J. Baran, J. Vannahme, H.J. Jakobsen, J. Skibsted, Single-crystal growth and characterization of disilver(I) monofluorophosphate(V), Ag_2PO_3F: crystal structure, thermal behavior, vibrational spectroscopy, and solid-state ^{19}F, ^{31}P, and ^{109}Ag MAS NMR spectroscopy, Inorg. Chem. 46 (2007) 801–808.
[6] E.R. Andrew, M. Firth, A. Jasinski, P.J. Randall, Resolved spin multiplets in the nuclear magnetic resonance spectra of solids, Phys. Lett. 31 (1970) 446–447.
[7] T. Krahl, M. Ahrens, G. Scholz, D. Heidemann, E. Kemnitz, Structure of $(NH_4)_3GaF_6$ investigated by multinuclear magic-angle spinning NMR Spectroscopy In Comparison with Rietveld refinement, Inorg. Chem. 47 (2008) 663–670.
[8] M. Gerken, P. Hazendonk, A. Iuga, J. Nieboer, M. Tramsek, E. Goreshnik, B. Zemva, S. Zheng, J. Autschbach, Solid-state NMR spectroscopic study of coordination compounds of XeF_2 with metal cations and the crystal structure of $[Ba(XeF_2)_5][AsF_6]_2$, Inorg. Chem. 46 (2007) 6069–6077.
[9] L.S. Du, R.W. Schurko, K.H. Lim, C.P. Grey, A solid-state ^{93}Nb and ^{19}F NMR spectroscopy and X-ray diffraction study of potassium heptafluoroniobate(V): characterization of ^{93}Nb, ^{19}F coupling, and fluorine motion, J. Phys. Chem. A 105 (2001) 760–768.
[10] D. Massiot, F. Fayon, M. Deschamps, S. Cadars, P. Florian, V. Montouillout, N. Pellerin, J. Hiet, A. Rakhmatullin, C. Bessada, Detection and use of small *J* couplings in solid state NMR experiments, C. R. Chim. 13 (2010) 117–129.
[11] G. Scholz, T. Krahl, M. Ahrens, C. Martineau, J.-Y. Buzaré, C. Jäger, E. Kemnitz, ^{115}In and ^{19}F MAS NMR study of $(NH_4)_3InF_6$ phases, J. Fluorine Chem. 132 (2011) 244–249.
[12] S.P. Gabuda, V.Ya. Kavun, S.G. Kozlova, V.V. Tveskikh, Structure of hexafluorostannate ion $[SnF_6]^{2-}$: the ^{119}Sn and ^{19}F NMR MAS-spectroscopic studies and *ab initio* calculations, Russ. J. Coord. Chem. 29 (2003) 3–7.
[13] T. Bräuniger, St. Ghedia, M. Jansen, Covalent bonds in α-SnF_2 monitored by *J*-couplings in solid-state NMR spectra, Z. Anorg. Allg. Chem. 636 (2010) 2399–2404.
[14] R.E.J. Sears, Q.Zh. Guo, H.J. Mackey, Electron-coupled nuclear spin-spin interactions in cubic PbF_2 and the ^{19}F chemical shift, J. Chem. Phys. 80 (1984) 5448–5452.
[15] F. Wang, C.P. Grey, High-resolution solid state ^{19}F MAS NMR study of ionic motion in α-PbF_2, J. Am. Chem. Soc. 117 (1995) 6637–6638.
[16] F. Wang, C.P. Grey, A 1- and 2-D ^{19}F MAS NMR study of fluoride-ion mobility in α-PbF_2, J. Am. Chem. Soc. 120 (1998) 970–980.
[17] C. Martineau, F. Fayon, C. Legein, J.-Y. Buzaré, G. Silly, D. Massiot, Accurate heteronuclear *J*-coupling measurements in dilute spin systems using the multiple-quantum filtered *J*-resolved experiment, Chem. Commun. (2007) 2720–2722.
[18] C. Martineau, F. Fayon, C. Legein, J.-Y. Buzaré, D. Massiot, M. Body, F. Goutenoire, Structure determination of β-Pb_2ZnF_6 by coupling multinuclear solid state NMR, powder XRD and ab initio calculations, Dalton Trans. 44 (2008) 6150–6158.
[19] C. Martineau, F. Fayon, C. Legein, J.-Y. Buzaré, F. Goutenoire, E. Suard, Neutron powder diffraction, multinuclear, and multidimensional NMR structural investigation of $Pb_5Ga_3F_{19}$, Inorg. Chem. 47 (2008) 10895–10905.
[20] J.M. Griffin, J.R. Yates, A.J. Berry, S. Wimperis, S.E. Ashbrook, High-resolution ^{19}F MAS NMR spectroscopy: structural disorder and unusual *J* couplings in a fluorinated hydroxy-silicate, J. Am. Chem. Soc. 132 (2010) 15651–15660.
[21] M. Deschamps, F. Fayon, S. Cadars, A.L. Rollet, D. Massiot, ^1H and ^{19}F ultrafast MAS double-quantum single-quantum NMR correlation experiments with the dipolar homonuclear homogeneous Hamiltonian, Phys. Chem. Chem. Phys. 13 (2011) 8024–8030.
[22] L. Yu, W. Pang, L. Li, Synthesis and structure of a novel microporous crystal $AlPO4_4$-CJ2, J. Solid State Chem. 87 (1990) 241–244.
[23] S.T. Wilson, B.M. Lok, C.A. Messina, T.R. Cannan, E.M. Flanigen, Aluminophosphate molecular sieves: a new class of microporous crystalline inorganic solids, J. Am. Chem. Soc. 104 (1982) 1146–1147.
[24] G. Férey, T. Loiseau, P. Lacorre, F. Taulelle, Oxyfluorinated microporous compounds I. Crystal structure of $(NH_4)_{0.93}(H_3O)_{0.07}GaPO_4(OH)_{0.5}F_{0.5}$; reexamination of the structure of $AlPO_4$-CJ2, J. Solid State Chem. 105 (1993) 179–190.
[25] B.M. Fung, A.K. Khitrin, K. Ermolaev, An improved broadband decoupling sequence for liquid crystals and solids, J. Magn. Reson. 142 (2000) 97–101.
[26] S.R. Hartmann, E.L. Hahn, Nuclear double resonance in the rotating frame, Phys. Rev. 128 (1962) 2042–2053.
[27] A. Pines, M.G. Gibby, J.S. Waugh, Proton-enhanced nuclear induction spectroscopy. A method for high resolution NMR of dilute spins in solids, J. Chem. Phys. 56 (1972) 1776–1777.
[28] G. Metz, X. Wu, S.O. Smith, Ramped-amplitude cross polarization in magic-angle-spinning NMR, J. Magn. Reson. A 110 (1993) 219–227.
[29] L. Delevoye, C. Fernandez, C.M. Morais, J.P. Amoureux, V. Montouillout, J. Rocha, Double-resonance decoupling for resolution enhancement of ^{31}P solid-state MAS and ^{27}Al–^{31}P MQHETCOR NMR, Solid State Nucl. Magn. Reson. 22 (2002) 501–512.
[30] A. Lesage, D. Sakellariou, S. Steuernegel, L. Emsley, Carbon–proton chemical shift correlation in solid-state NMR by through-bond multiple-quantum spectroscopy, J. Am. Chem. Soc. 120 (1998) 13194–13201.
[31] H. Geen, J.J. Titman, J. Gottwald, H.W. Spiess, Solid-state proton multiple-quantum NMR spectroscopy with fast magic angle spinning, Chem. Phys. Lett. 227 (1994) 79–86.
[32] D. States, R. Haberkorn, D. Ruben, A two-dimensional nuclear overhauser experiment with pure absorption phase in four quadrants, J. Magn. Reson. 48 (1982) 286–292.
[33] D. Massiot, F. Fayon, M. Capron, I. King, S. Le Calvé, B. Alonso, J.O. Durand, B. Bujoli, Z. Gan, G. Hoatson, Magn. Reson. Chem. 40 (2002) 70–76.
[34] J. Schaefer, R.A. McKay, US Patent No. 5861748, 1999.
[35] J.A. Frydel, M. Krzystyniak, D. Pienkowski, M. Pietrzak, N. de Sousa Amadeu, T. Ratajczyk, K. Idzik, T. Gutmann, D. Tietze, S. Voigt, A. Fenn, H.H. Limbach, G. Buntkowsky, Efficient design of multituned transmission line NMR probes: the electrical engineering approach, Solid State Nucl. Magn. Reson. (2011), doi:10.1016/j.ssnmr.2011.01.001.
[36] B.H. Meier, Personal Communication of the External $^{19}F/^1H$ Tuning Splitter Circuit Proposed by J. van Os, University of Nijmegen.
[37] M. Bechmann, K. Hain, C. Marichal, A. Sebald, X–{^1H; ^{19}F} triple resonance with a X–{^1H} CP MAS probe and characterisation of a ^{29}Si–^{19}F spin pair, Solid State Nucl. Magn. Reson. 23 (2003) 50–61.
[38] H. Zeiger, US Patent 6307,371 B1, October 23, 2001.
[39] F. Taulelle, M. Pruski, J.P. Amoureux, D. Lang, A. Bailly, C. Huguenard, M. Haouas, C. Gérardin, T. Loiseau, G. Férey, Isomerization of the prenucleation building unit during crystallization of $AlPO_4$-CJ2: an MQMAS, CP-MQMAS, and HETCOR NMR study, J. Am. Chem. Soc. 121 (1999) 12148–12153.
[40] F. Bloch, A. Siegert, Magnetic resonance for nonrotating fields, Phys. Rev. 57 (1940) 522–527.
[41] Q. Wang, B. Hu, F. Fayon, J. Trébosc, C. Legein, O. Lafon, F. Deng, J.P. Amoureux, Double-quantum ^{19}F–^{19}F dipolar recoupling at ultra-fast magic angle spinning NMR: application to the assignment of ^{19}F NMR spectra of inorganic fluorides, Phys. Chem. Chem. Phys. 11 (2009) 10391–10396.
[42] M. Pruski, D.P. Lang, C. Fernandez, J.P. Amoureux, Multiple-quantum magic-angle spinning NMR with cross-polarization: spectral editing of high-resolution spectra of quadrupolar nuclei, Solid State Nucl. Magn. Reson. 7 (1997) 327–331.
[43] F. Taulelle, Clipping a network into a crystal, Solid State Sci. 3 (2001) 795–800.
[44] M. Fechtelkord, H. Behrens, F. Holtz, J.L. Bretherton, C.A. Fyfe, L.A. Groat, M. Raudsepp, Influence of F content on the composition of Al-rich synthetic phlogopite: part II. Probing the structural arrangement of aluminium in tetrahedral and octahedral layers by ^{27}Al MQMAS and $^1H/^{19}F$–^{27}Al HETCOR and REDOR experiments, Am. Mineral. 88 (2003) 1046–1051.
[45] J. Dutour, N. Guillou, C. Huguenard, F. Taulelle, C. Mellot-Draznieks, G. Férey, Chiolite, a case study for combining NMR crystallography, diffraction and structural simulation, Solid State Sci. 6 (2004) 1059–1067.
[46] S.H. Wang, S.M. De Paul, L.M. Bull, High-resolution heteronuclear correlation between quadrupolar and spin-1/2 nuclei using multiple-quantum magic-angle spinning, J. Magn. Reson. 125 (1997) 364–368.
[47] J.W. Wiench, M. Pruski, Probing through bond connectivities with MQMAS NMR, Solid State Nucl. Magn. Reson. 26 (2004) 51–55.
[48] J.P. Amoureux, J. Trebosc, J. Wiench, M. Pruski, HMQC and refocused-INEPT experiments involving half-integer quadrupolar nuclei in solids, J. Magn. Reson. 184 (2007) 1–14.
[49] M. Feike, D. Demco, R. Graf, J. Gottwald, S. Hafner, H.W. Spiess, Broadband multiple-quantum NMR spectroscopy, J. Magn. Reson. Ser. A 122 (1996) 214–221.

[50] B. Hu, Q. Wang, O. Lafon, J. Trébosc, F. Deng, J.P. Amoureux, Robust and efficient spin-locked symmetry-based double-quantum homonuclear dipolar recoupling for probing ^{1}H–^{1}H proximity in the solid-state, J. Magn. Reson. 198 (2009) 41–48.

[51] T.M. Alam, J.S. Clawson, F. Bonhomme, S.G. Thoma, M.A. Rodriguez, S. Zheng, J. Autschbach, A solid-state NMR, X-ray diffraction, and ab initio investigation into the structures of novel tantalum oxyfluoride clusters, J. Chem. Mater. 20 (2008) 2205–2217.

[52] C. Martineau, C. Legein, J.-Y. Buzaré, F. Fayon, On the assignment of ^{19}F MAS NMR spectra of fluoroaluminates using through-space spectral edition of ^{19}F–^{27}Al and ^{19}F–^{19}F connectivities, Phys. Chem. Chem. Phys. 11 (2009) 950–957.

[53] A. Cadiau, C. Martineau, M. Leblanc, V. Maisonneuve, A. Hémon-Ribaud, F. Taulelle, K. Adil, $ZnAlF_5$·[TAZ]: an Al fluorinated MOF of MIL-53(Al) topology with cationic $\{Zn(1,2,4\ triazole)\}^{2+}$ linkers, J. Mater. Chem. 21 (2011) 3949–3951.

[54] C. Martineau, F. Fayon, M.R. Suchomel, M. Allix, D. Massiot, F. Taulelle, Structure resolution of $Ba_5Al_3F_{19}$ and investigation of fluorine ion dynamics by synchrotron powder diffraction, variable temperature solid-state NMR and quantum computations, Inorg. Chem. 50 (2011) 2644–2653.

[55] K. Pervushin, R. Riek, G. Wider, K. Wütrich, Attenuated T_2 relaxation by mutual cancellation of dipole–dipole coupling and chemical shift anisotropy indicates an avenue to NMR structures of very large biological macromolecules in solution, Proc. Nat. Acad. Sci. USA 94 (1997) 12366–12371.